Supplementary Information

Abhilash Sahoo,[†] Hongcheng Xu,[†] and Silvina Matysiak[*,†,‡]

†*Biophysics Program, Institute of Physical Science and Technology, University of Maryland, College Park, MD*

‡*Fischell Department of Bioengineering, University of Maryland, College Park, MD*

E-mail: matysiak@umd.edu

Methods

Bonded and nonbonded interaction parameters

The bonded interaction parameters of the peptide molecule are listed in Table S1. Some modification are made from previous WEPPRO model.[1] The backbone dummy angle (D-BB-D) was modified from 0 degree to 180 degrees to mimic the structure of typical peptide bonds. The modification increases the dipole moment of polarizable peptide backbone beads and stabilize the formation of secondary structure as in agreement with quantum mechanical calculations.[2] The SC1-SC2 bonds and BB-SC1-SC2 angles were added into the model because amino acids such as lysine, phenylalanine, and glutamate have two sidechain beads instead of one. The original BB-BB-SC1 angles were removed from the model and replaced by non-bonded interactions between backbone beads to sidechain beads on adjacent amino acids. Similar to the original implementation of this model. no external dihedral potential has been used to maintain the secondary structure of the peptide.[1]

The non-bonded interactions were mostly adapted from our previous WEPMEM model.[3] There are a few modifications made in this work to improve the characterization of peptide

Table S1: Bond and angle parameters in WEPPRO model. BB: Backbone bead, D: dummy particle, SC1: Sidechain 1 bead, SC2: Sidechain 2 bead.

bonds	R_{bond} (nm)	K_{bond} (kJ mol^{-1} nm^{-2})
BB-BB	0.385	7500
BB-D	0.14	5000
BB-SC1	0.25	5000
SC1-SC2	0.28	5000
angles	$\theta_0(deg)$	K$_{angle}$ (kJ mol^{-1})
D-BB-D	180	7.2
BB-BB-BB	109	75
BB-SC1-SC2 (LYS, PHE)	151	25
BB-SC1-SC2 (GLU)	180	25

secondary structure in membraneous environment. The LJ interactions between peptide backbone bead type P5 (BB) and charged beads (Qd/Qa) were changed from 4 kJ/mol to 5.32 kJ/mol to avoid overbinding. Also, if the interaction between hydrophobic beads and water beads are too low, the hydrophobic beads tend to aggregate in the aqueous environment. To maintain the intricate balance between apolar-water and apolar-apolar interactions, the interactions between hydrophobic sidechain bead type C1 and water bead type POL were modified from 0.2 kJ/mol to 1.0 kJ/mol.

Table S2: Non-bonded Lennard-Jones (LJ) interaction strengths in WEPPRO model. Unit of interaction strength (ϵ) is in kJ/mol. The radius (σ) of all LJ interactions is 4.7Å.

Beads	BB (P5)	H1 (C1)	H2 (C3)	C$^+$ (Qd)	C$^-$ (Qa)	Water (POL)
BB (P5)	5.0	2.0	2.7	5.32	5.32	4.75
H1 (C1)	2.0	3.5	3.5	2.3	2.3	1.0
H2 (C3)	2.7	3.5	3.5	2.7	2.7	2.7
C$^+$ (Qd)	5.32	2.3	2.7	3.5	4.0	5.0
C$^-$ (Qa)	5.32	2.3	2.7	4.0	3.5	5.0
Water (POL)	4.75	1.0	2.7	5.0	5.0	4.0

Simulations in aqueous solution

Aβ 16-22 organizes into stable layered beta sheets in aqueous solution. These beta sheets are stabilized by a hydrophobic patch formed between them. We validated our Aβ 16-22 peptide model using 12 peptide simulations in aqueous solution. Similar to other reported experimental and simulation[4,5] based observations, peptides in our 500 ns simulation organized into stable, layered beta sheet rich structures.

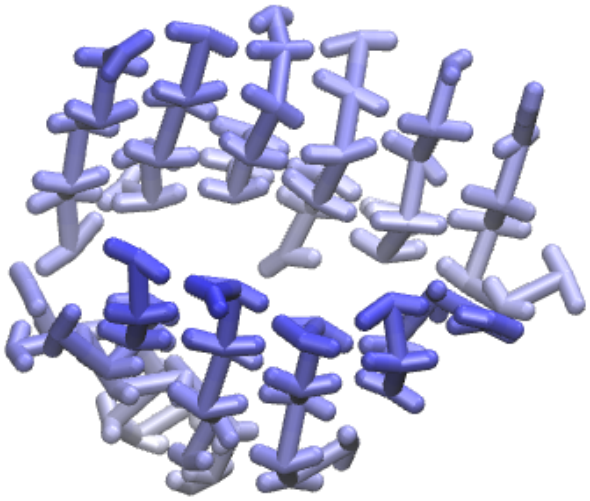

Figure S1: Aggregated structure of 12 solvated peptide in aqueous solution

Algorithm for peptide absorption

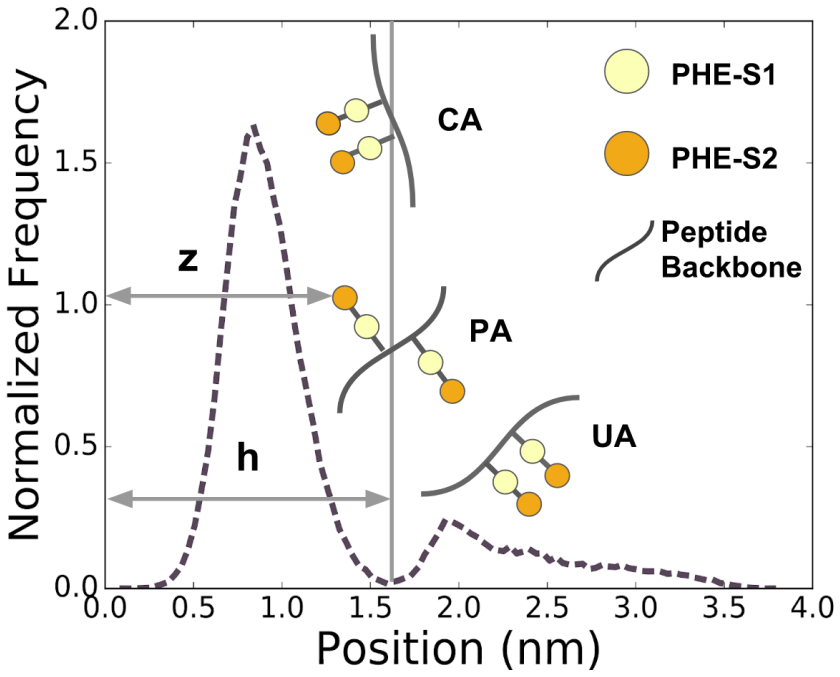

Figure S2: Graphical description of peptide absorption algorithm. The gray line marks the average bilayer height determined by relative position of six nearest PO4 beads along bilayer normal. The dashed curve presents number-density distribution of PHE-S2 along bilayer normal from bilayer center for reference.

Radial distribution Functions

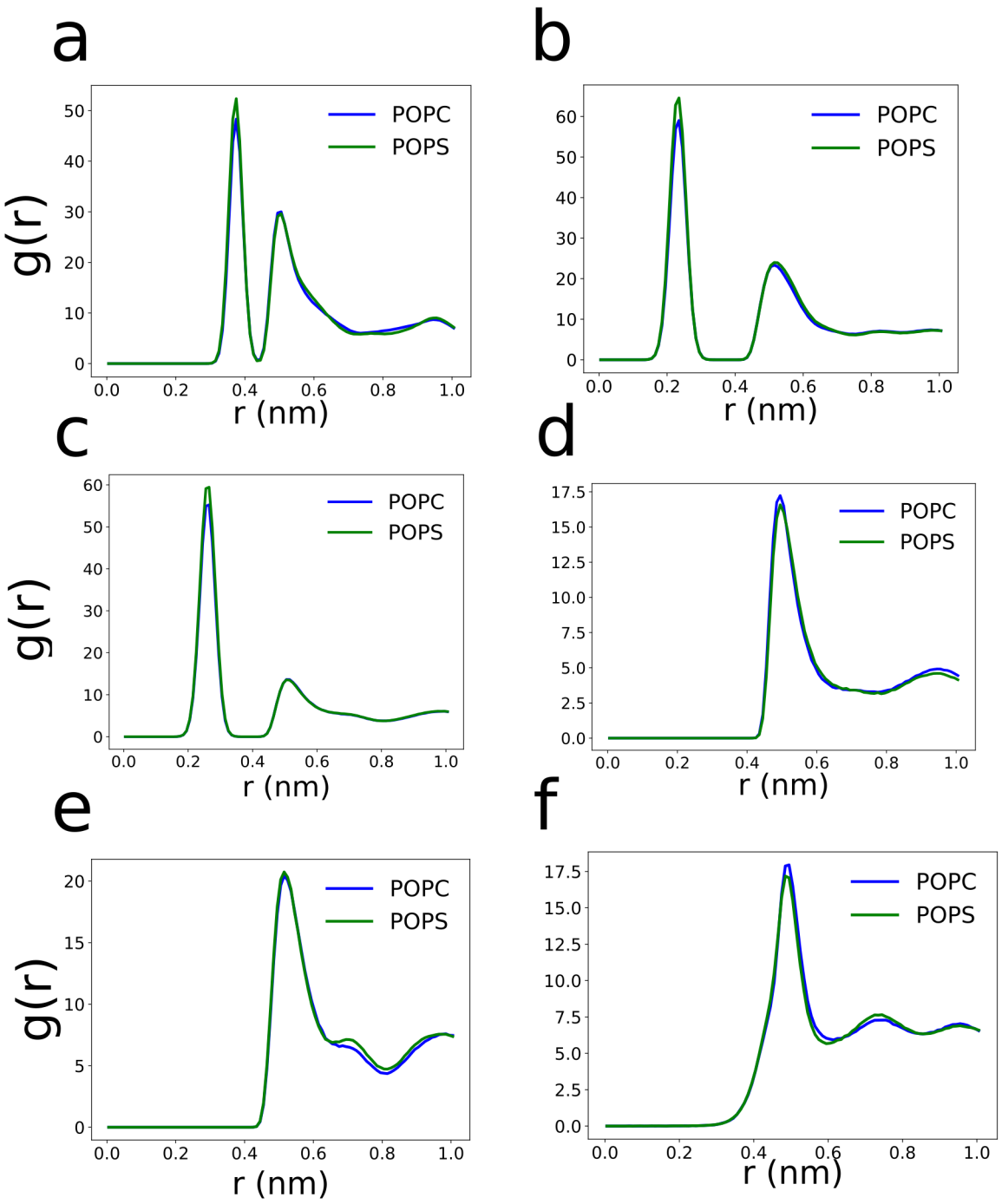

Figure S3: Radial distribution functions between different peptide beads. a) BB-BB, b) BB-S1 c) S1-S2, c) S2-S2, d) BB-S2, e) S1-S1

Variable residue-wise peptide insertion

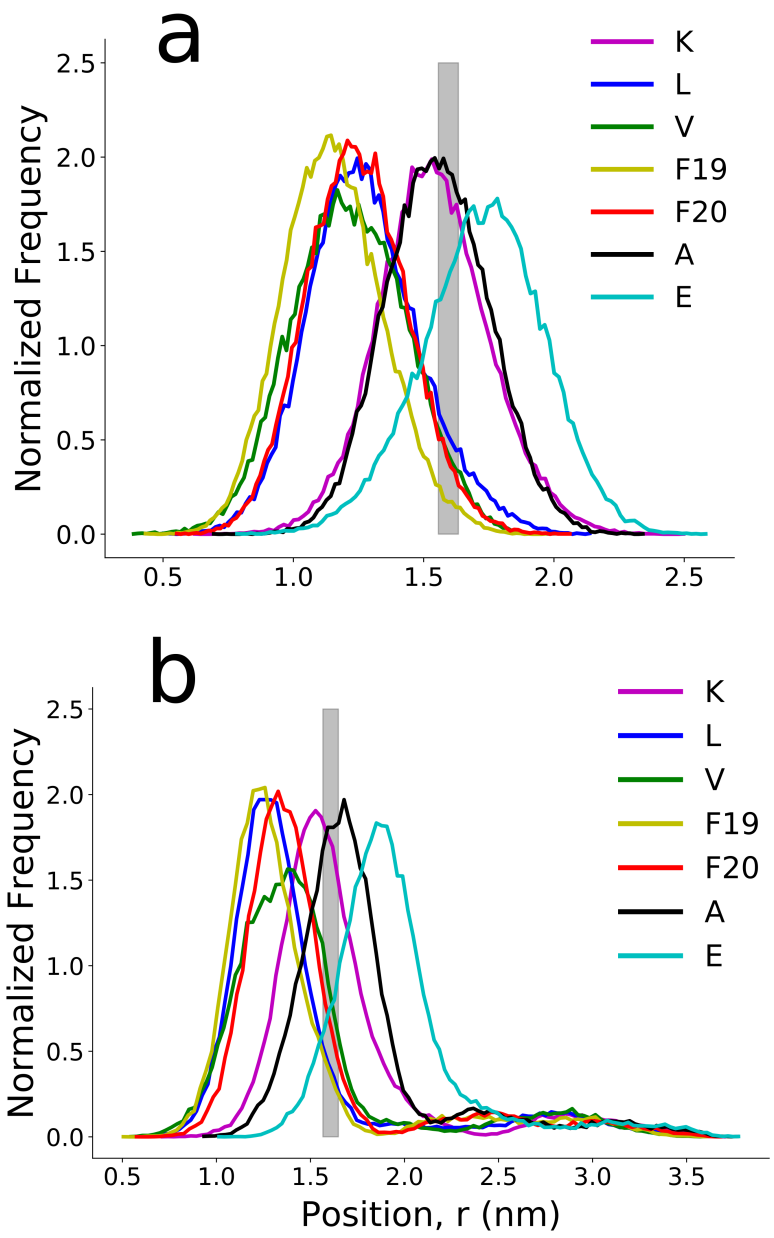

Figure S4: Residue-wise insertion of Backbone beads (BB) into different membranes. a)POPC bilayer; b)POPS bilayer. The gray region describes the average location of bilayer headgroup (PO4). The presented results have been averaged over both replica-simulations.

Size of peptide clusters

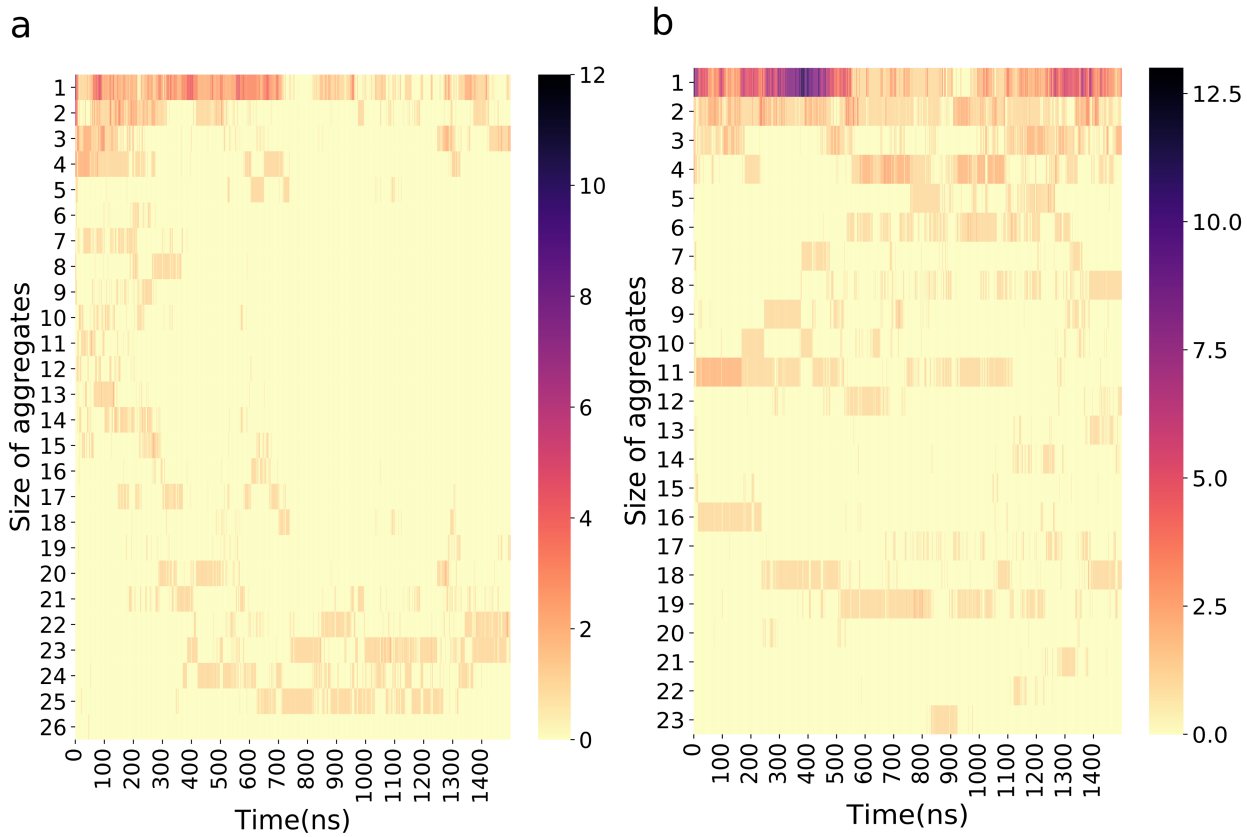

Figure S5: Variation of size of peptide aggregates with time. The colors of heatmap correspond to frequency of particular sized aggregate. a)POPC bilayer; b)POPS bilayer. The presented results have been averaged over both replica-simulations.

All-atom simulations

We compared the resultant shapes of peptides in our coarse grained membrane-peptide simulations with single Aβ 16-22 peptide membrane atomistic simulations. The simulations were initiated with two distinct initial conformations for both POPC and POPS membrane systems to attempt a wider sampling of conformational space. The initial membrane-peptide conformation with one Aβ 16-22 peptide — created with Molfacture plugin of VMD, 40 lipid molecules per leaflet and 60 TIP3P water molecules per lipid was assembled using CHARMM-GUI membrane builder[6] into tetragonal ($x = y \neq z$) boxes. In the initial conformation, peptide was placed at the headgroup (center of geometry 2.5 nm away from bilayer center) of the membrane to have a very fast absorption. MD simulations were carried out using GROMACS 5.0.4[7] with CHARMM36 forcefield.[8] Standard six step equillibration CHARMM-GUI protocol was used with exception of the last step, where peptide was restrained along z-direction (through a position restraint placed at F (Phenylalanine) backbone (atoms N and C)) and bilayer was allowed to relax to area per lipid comparable to CG simulations (95 $\mathring{A}^2$) over 20 ns at constant surface tension. The position restraint on peptide is then released and the systems are simulated for 80 ns each. We used a surface-tension type pressure coupling with to maintain a constant area per lipid throughout the simulation. Short-range non-bonded interactions were treated with a force-based switching scheme (from 0.8 nm to 1.2 nm) and long range electrostatic over 1.2 nm in the system were treated by the Particle Mesh Ewald (PME) method. The hydrogen bonds were constrained using LINCS[9] and the simulation time step was set at 2 fs.

The simulations were analyzed by in-house developed scripts and analyzed with VMD. The distribution of end-to-end distance of peptides over multiple simulations (for last 60 ns) are provided in Figure S6. The last 60 ns were chosen for analyses based on low variation in z-direction (standard deviation < 2 $\mathring{A}$) of peptide backbone's center of geometry. We defined the end-to-end distance as the distance between terminal nitrogen (N) of K which is a part of peptide backbone and terminal carbon (C) of E which is also a part of peptide backbone.

The plot confirms that peptides in POPS are in general more elongated than peptides in POPC membranes. The representative snapshots of peptides in Figure S6 also presents the "U" shape that was characterized in our coarse grained simulations. In the first simulation (simulation 1) with POPC membrane, the system captured a "O"-like conformation for the peptides (similar to observed conformation in coarse grained simulations) due to interaction of flanking charged residues (K and E).

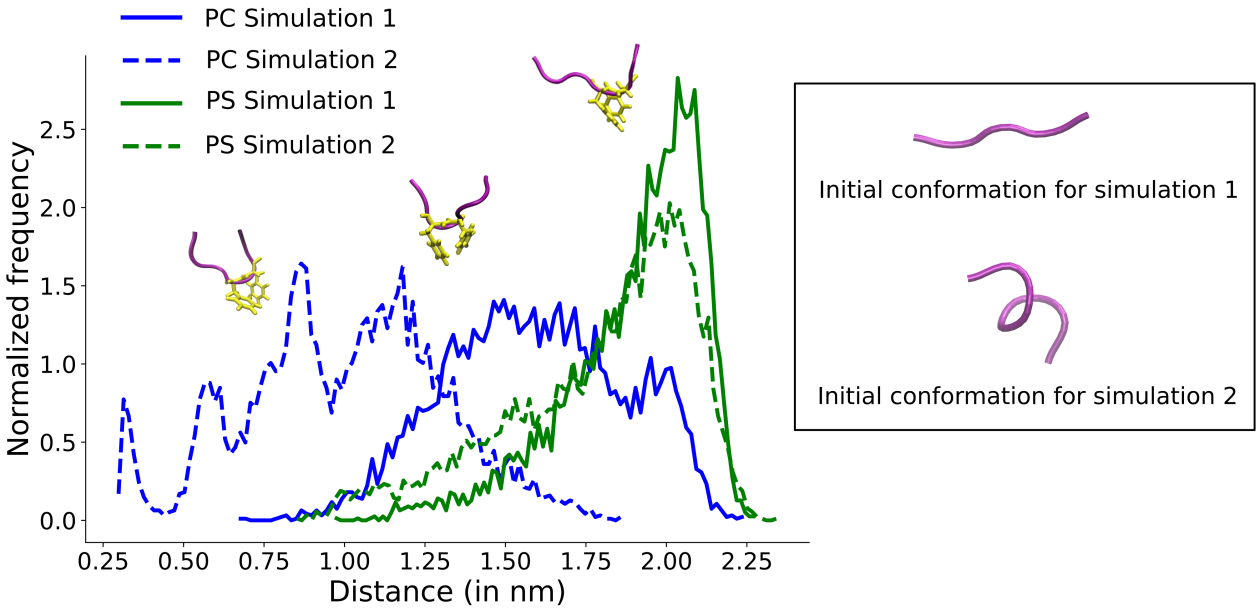

Figure S6: Distribution of peptide end-to-end distances over different atomistic simulations. The end-to-end distance is defined as the distance between terminal nitrogen (N) of K which is a part of peptide backbone and terminal carbon (C) of E which is also a part of peptide backbone. Color scheme of VMD snapshots: Purple - Peptide backbone, Yellow - F (Phenylalanine)

Peptide simulation with 96 peptides

After 1.5 micro-second of simulation, 48 more peptides were added (new peptide to lipid ratio of 2:5) to verify whether pre-formed oligomers can act as nucleating agents. Figure S7 presents snapshots of peptide aggregation after 500 ns of extended simulation and bar graphs comparing size of peptide clusters before and after 500 ns of extended simulation time. The

increase in size of peptide cluster confirmed that pre-existing oligomers can act as nucleating agents. In addition, similar to reported results in aggregation kinetics (Figure 3e - main text), we found there were more singlet peptides (present without association with other peptides) in POPS (six) as compared to POPC (one). One small oligomer (of 4 monomers) was incorporated into a larger aggregation in POPS.

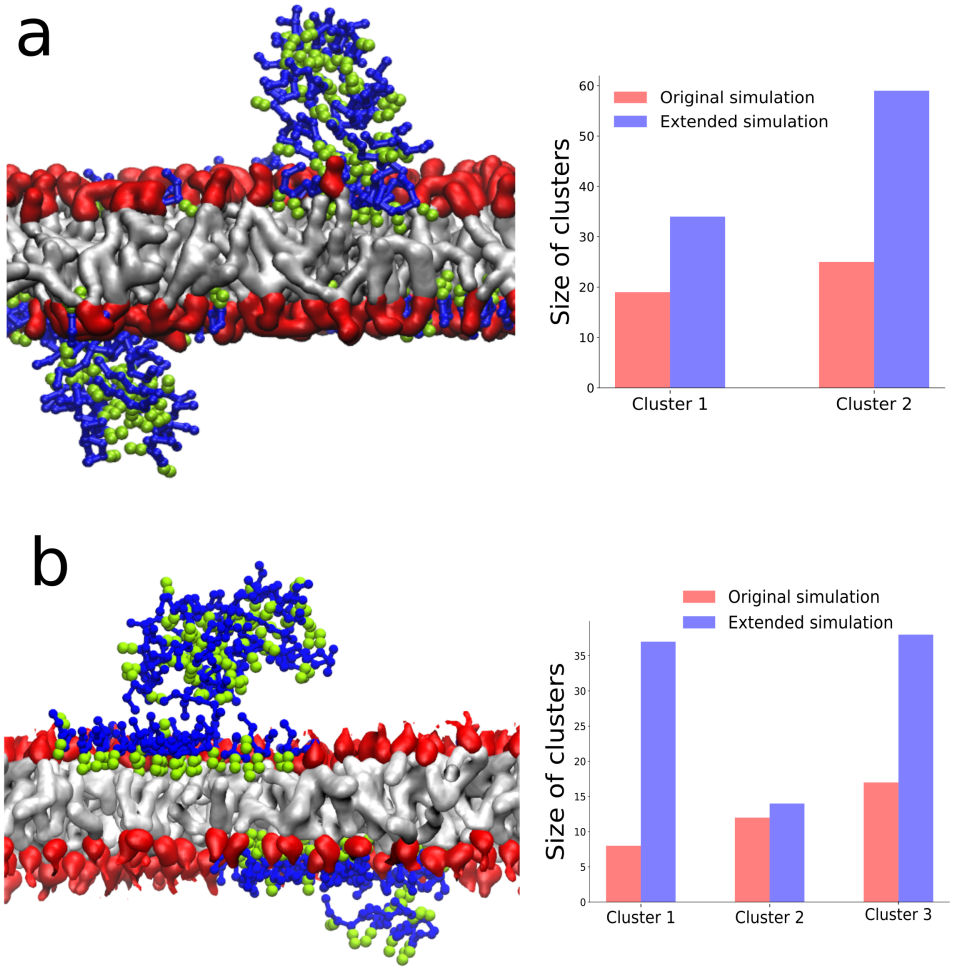

Figure S7: a) Sanpshot of peptide aggregation on POPC bilayer at the end of extended simulation. b) Snapshot of peptide aggregation on POPS bilayer at the end of extended simulation. Coloring scheme of VMD snapshots: Light green beads - Sidechains of Phenylalanines (F); Blue beads - Peptide backbones; Red region - Polar lipid headgroup; White region - Hydrophobic alkyl tails (Lipids). *Right*-Increase in size of clusters by addition of 48 new peptides and extension of simulation for POPC (a) and POPS (b). The size of initial cluster increased due to recruitment of peptides during 500 ns of extended simulation.

Simulation 1: Peptide-Membrane system

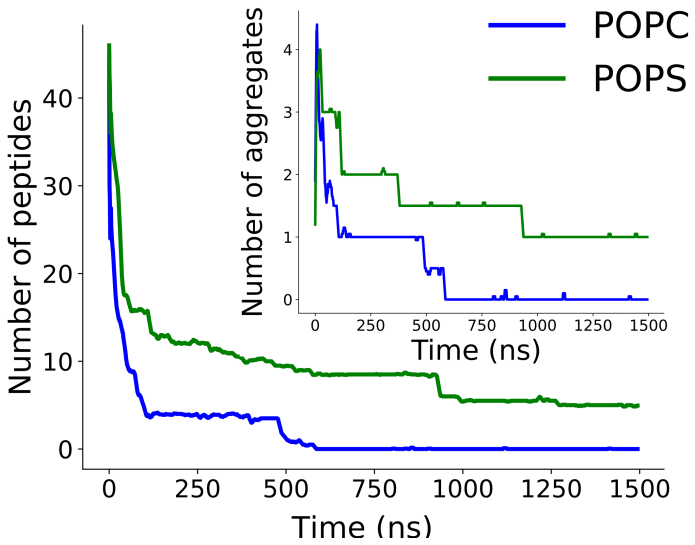

Figure S8: Variation of number of "unabsorbed peptides" with time. The variation of the number of partially absorbed aggregates has been provided as *inset*.

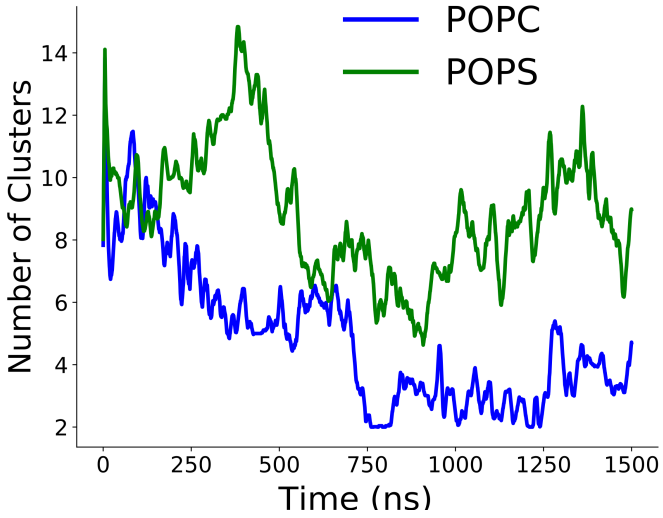

Figure S9: Variation in the number of Aβ 16-22 aggregates over time. Even connected components of size one (monomers) have been designated as a single cluster.

Figure S10: Variation of beta sheet fraction over time. Two peptides are categorized as part of beta sheet if they have an end-to-end length greater than 1 nm and atleast five dipole-dipole contacts.

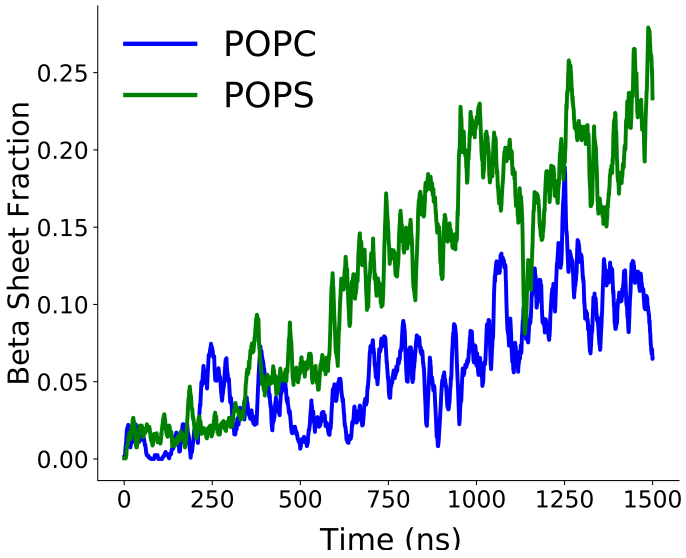

Simulation 2: Peptide-Membrane system

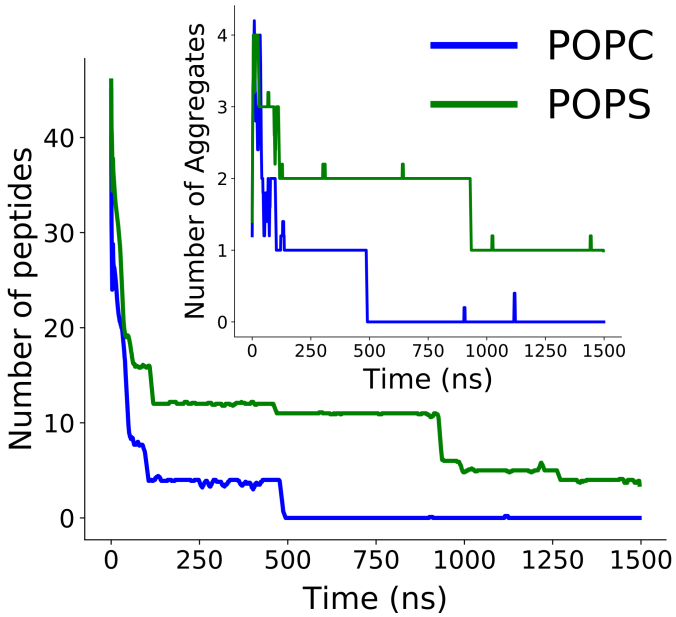

Figure S11: Variation of number of "unabsorbed peptides" with time. The variation of the number of partially absorbed aggregates has been provided as *inset*.

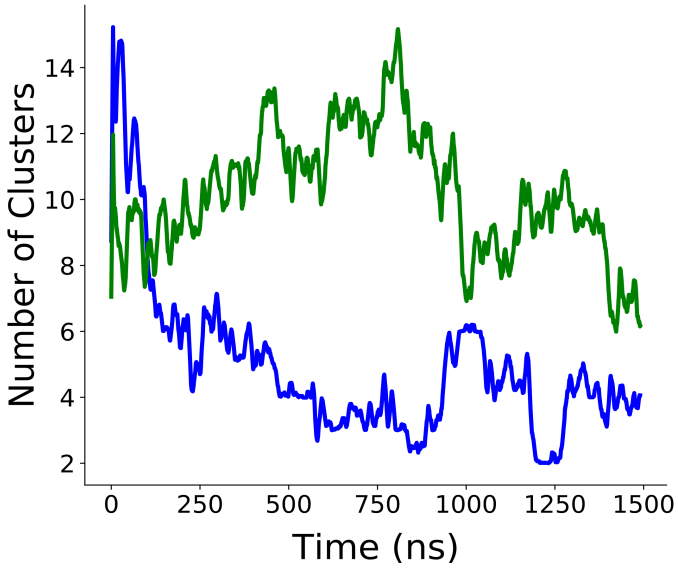

Figure S12: Variation in the number of Aβ 16-22 aggregates over time. Even connected components of size one (monomers) have been designated as a single cluster.

Figure S13: Variation of beta sheet fraction over time. Two peptides are categorized as part of beta sheet if they have an end-to-end length greater than 1 nm and atleast five dipole-dipole contacts.

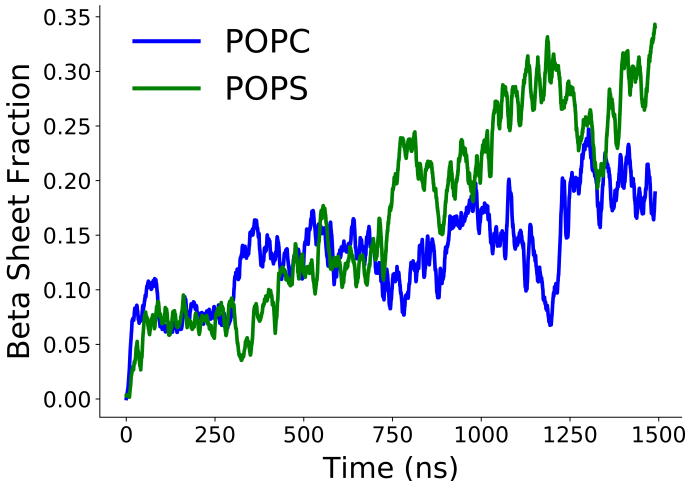

References

(1) Ganesan, S. J.; Matysiak, S. *J. Chem. Theory Comput.* **2014**, *10*, 2569–2576.

(2) Herrera, F. E.; Pantano, S. *J. Chem. Phys.* **2012**, *136*, 015103.

(3) Ganesan, S. J.; Xu, H.; Matysiak, S. *Phys. Chem. Chem. Phys.* **2016**, *18*, 17836–17850.

(4) Mehta, A. K.; Lu, K.; Childers, W. S.; Liang, Y.; Dublin, S. N.; Dong, J.; Snyder, J. P.; Pingali, S. V.; Thiyagarajan, P.; Lynn, D. G. *J. Am. Chem. Soc.* **2008**, *130*, 9829–9835.

(5) Lu, Y.; Derreumaux, P.; Guo, Z.; Mousseau, N.; Wei, G. *Proteins* **2009**, *75*, 954–63.

(6) Wu, E. L.; Cheng, X.; Jo, S.; Rui, H.; Song, K. C.; Dávila-Contreras, E. M.; Qi, Y.; Lee, J.; Monje-Galvan, V.; Venable, R. M.; Klauda, J. B.; Im, W. *J. Comput. Chem.* **2014**, *35*, 1997–2004.

(7) Abraham, M. J.; Murtola, T.; Schulz, R.; Páll, S.; Smith, J. C.; Hess, B.; Lindahl, E. *SoftwareX* **2015**, *1-2*, 19–25.

(8) Klauda, J. B.; Venable, R. M.; Freites, J. A.; O'Connor, J. W.; Tobias, D. J.; Mondragon-Ramirez, C.; Vorobyov, I.; MacKerell, A. D.; Pastor, R. W. *The journal of physical chemistry. B* **2010**, *114 23*, 7830–43.

(9) Hess, B.; Bekker, H.; Berendsen, H. J.; Fraaije, J. G. *J. Comput. Chem.* **1997**,